DOI: 10.13009/EUCASS2022-6138

Analysis of coolant flow and heat transfer in highly rough channels for LRE

Beatrice Latini ⋆ *Matteo Fiore*⋆ *and Francesco Nasuti*⋆†
⋆*Sapienza University of Rome*
Dipartimento di Ingegneria Meccanica e Aerospaziale, Via Eudossiana 18, Rome I-00184
beatrice.latini@uniroma1.it · matteo.fiore@uniroma1.it · francesco.nasuti@uniroma1.it
†Corresponding author

Abstract

The realization of thrust chambers for the new generation of liquid rocket engines is based on the increasingly popular additive layer manufacturing (ALM) techniques. Such techniques show advantages in terms of design flexibility, production costs and times, but at the same time, if used to manufacture tiny cooling channels lead to high relative surface roughness. In principle, the high roughness of channels is not necessarily unfavorable. In general, it is known to increase heat transfer at the cost of increased pressure loss. However, the correlation between the increase of friction and heat transfer changes at high roughness and the commonly used assumption for heat transfer prediction at low roughness may lead to order of magnitude errors if extended to high roughness channels. Therefore, special corrections must be introduced to have a reliable heat transfer prediction model, such as the one proposed in the present study for circular cross-section channels. The present correction of the Spalart-Allmaras one equation model for the closure of Reynolds averaged Navier-Stokes equations if of easy implementation and allows the user to predict realistic values of the convective heat transfer coefficient, in agreement with the correlations and experimental data reported in the literature.

1. Introduction

Cooling of thrust chamber walls, which is required because of the huge amount of power released in a relatively small volume, is one of the most challenging aspects of the design, realization, and testing of liquid propellant rocket engines (LRE). Among the different cooling techniques, the regenerative cooling system is the most employed because of its high efficiency. This technique uses one of the propellants on board, which flows through small channels surrounding the thrust chamber to cool the wall and keep it within the allowable range of temperatures that guarantee its resistance to the expected range of static, dynamic, and fatigue stresses. Additionally, in special cases [1, 2], the use of one of the propellants as a cooling medium allows to exploit the power taken by the coolant in the cooling system as the input power for gas turbines in expander cycles. Therefore, to ensure the engine operational life, predictions of the flow field and heat transfer in the cooling channels constitute an important part of the design process.

The prediction of pressure loss and heat transfer in cooling channels has been commonly and successfully achieved by one-dimensional models, at least as long as a liquid is flowing in reasonably smooth channels. However, channel wall roughness cannot be completely removed, so the effect of roughness, even when small, has to be included in modeling. Accordingly, even in the case of small roughness, a special model has been considered taking into account the different roles of roughness on friction and heat transfer [3, 4, 5]. Such a model intends to increasingly separate the heat transfer from the friction behavior as roughness increases.

It has been shown that, despite the small value, roughness modeling can play a significant role in wall temperature predictions [6]. Roughness, indeed, leads to an increase in friction and heat transfer, although heat transfer enhancement is less than the friction one because of the different physical phenomena [7, 8]. In fact, while the increase in friction is due to pressure forces acting on the roughness elements, there is no corresponding mechanism with respect to heat transfer. Although the heat transfer capacity of the fluid away from the wall is increased by the turbulence generated by roughness, heat can be transferred by eddy conductivity down to the plane of the roughness elements, but the rate of heat transport in the immediate neighborhood of the surface is controlled by molecular conductivity. Therefore, the Reynolds analogy, or the more general Chilton-Colburn analogy, no longer holds on rough surfaces, and the whole concept of analogous behavior between heat and momentum transfer breaks down at high roughness. Nevertheless, while the effects of roughness on momentum transport are well consolidated, the literature is less unitary

DOI: 10.13009/EUCASS2022-6138

about the increase in heat transfer. Attempts to directly correlate heat transfer and friction factor coefficients have been reported for over a century [4, 7, 8, 9] and are the basis for today development [10, 11].

The importance of correct modeling of roughness in cooling channels is increasing nowadays, driven by two main different reasons: one is the introduction of additive layer manufacturing techniques which typically come with the realization of high-roughness channels; the other is the use of a coolant less known and more peculiar than hydrogen and water, namely methane.

In fact, on the one hand, metal additive layer manufacturing (ALM) is becoming one of the key technologies for the realization of cooling channels of increasing complexity and efficiency for regeneratively cooled thrust chambers [12, 13]. Inherent in ALM processes is the large surface finish, which, when considering mini-channels (with hydraulic diameter less than 3 mm), often implies that the absolute and relative roughness are orders of magnitude higher than that considered in conventional designs.

On the other hand, methane has been proposed for different rocket engines and different engine cycles, all of them using it as the coolant in the regenerative cooling system, followed by injection into the combustion chamber or diversion to a turbine to provide power to an expander cycle engine [14, 15, 16, 17, 18]. However, methane has a lower thermal capacity with respect to hydrogen, thus poorer cooling performance, but still high enough to be considered among the candidate fuels for expander cycles [1, 2, 15, 19, 18]. It is interesting to note that, at the cost of high pressure loss, high roughness can be considered as a design option with a benign effect on the performance of the cooling system, either for better cooling of walls or to extract more power to be used in the turbine.

Moreover, recent studies on heat transfer deterioration, which may occur while heating liquid propellants, have shown that wall roughness has a mitigating effect with respect to heat transfer deterioration, especially at high roughness. In particular, the presence of roughness can lead to a significant reduction of the peak wall temperature and smooths the transcritical process that the coolant may undergo in the cooling channels [2, 20, 21, 22]. Here, it is also worth mentioning that methane can experience a significant change in properties along the channel, as shown by a typical evolution of the Prandtl number depicted in Fig. 1.

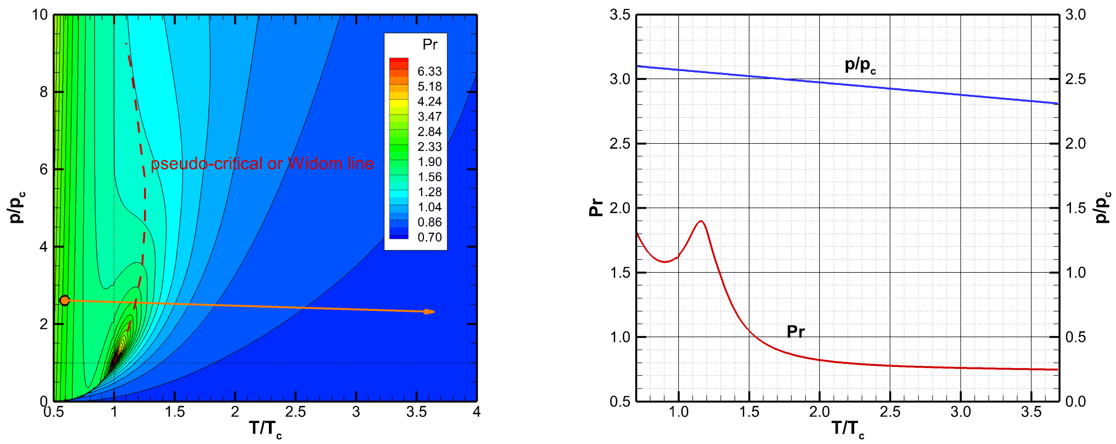

Figure 1: Possible Prandtl number evolution in LRE cooling channels

In this framework, numerical predictions of flow in high-roughness LRE cooling channels become of paramount importance during the design phase. Among the flow models used as a support to the engine design phase, Reynolds averaged Navier-Stokes (RANS) equation solvers play an important role, often resulting in a good compromise between fidelity in reproducing turbulent flow phenomena and computational cost. Originally, RANS approaches do not foresee boundary conditions to take into account for wall roughness; however, different models have been developed in the years mainly focused on a suitable reproduction of wall friction. At present, the most common approaches to account for wall roughness in RANS numerical simulations, are based on the *equivalent sand grain approach*. This approach links the real roughness to an idealized equivalent sand grain roughness, with reference to Nikuradse's experiments [23, 24, 25]. The roughness effect is mimicked by increasing the turbulent eddy viscosity in the wall region to obtain higher levels of skin friction and heat transfer. Although this approach has the advantage of using the same set of equations as for flow over smooth surfaces and the equivalent sand grain roughness heights can be deduced through pressure drop measurements, it preserves the Reynolds analogy with a consequent overestimation of the convective heat transfer increase, especially in the case of high roughness level. Therefore, on this basis, it can only work at low roughness as there is no model to reproduce the difference between skin friction and heat transfer increase at

DOI: 10.13009/EUCASS2022-6138

high roughness. Accordingly, a suitable model able to take into account this different behavior must be introduced. This has been done by Aupoix, who developed a modification of Spalart-Allmaras one-equation turbulence model for external flows[26]. Following the same approach, the present study proposes an extension and calibration to internal flows of the high-roughness correction of the Spalart-Allmaras model originally developed for external flows in [26]. More specifically, the aim is to improve RANS model predictions in LRE cooling channels, by developing a thermal correction able to take into account the role of high roughness [27]. Because of the limited amount of experimental data, the proposed model is based on the correlation of Dipprey and Sabersky for heat transfer on fully rough surfaces and validated for circular cross-section pipes with constant property flow.

The paper is organized as follows. The effect of wall roughness on skin friction and heat transfer and its modeling is reviewed in Section 2. In Section 3 the numerical model and the formulation of the proposed correction are presented. Section 4 is dedicated to model calibration. The test case employed to perform RANS simulations is described and the grid convergence results with the basic roughness correction are illustrated. Then, the procedure adopted to calibrate the thermal correction and its general expression are described. Finally, results are presented and discussed in Section 5.

2. Wall Roughness Effects and Modeling

Turbulent flows over rough surfaces have been studied since the 19th century, as roughness can be encountered in a wide variety of engineering applications: pipe casting, erosion of gas turbine blades, ice accretion of aircraft, re-entry vehicle nosetips [26, 28, 29, 30].

The first main work on roughness, which still constitutes a reference, is due to Nikuradse [23], who investigated a water flow inside a pipe roughened with a calibrated sand grain. Through his experiments, he evidenced three flow regimes according to the sand grain height expressed in wall variables, h_s^+, also known as roughness Reynolds number:

$$h_s^+ = \frac{u_\tau h_s}{\nu} \tag{1}$$

where h_s is the sand grain height, $u_\tau = \sqrt{\tau_w/\rho}$ the friction velocity, ρ the fluid density, ν the fluid kinematic viscosity and τ_w the wall shear stress. The three flow regimes are known as: hydraulically smooth regime ($h_s^+ < 3.5$); transitional regime ($3.5 < h_s^+ < 68$); and fully rough regime ($h_s^+ > 68$). In particular, in fully rough conditions, the height of the roughness elements definitely exceeds the laminar sublayer thickness and the friction factor f becomes independent of the Reynolds number and is only a function of the relative pipe roughness h_s/D, where D is the pipe diameter. Nikuradse also pointed out that, regarding the velocity profile in terms of the nondimensional wall variables $u^+ = u/u_\tau$ and $y^+ = yu_\tau/\nu$ where y is the distance from the wall, the logarithmic region still exists but is shifted by the quantity ΔU^+, as shown in Fig. 2.

Near the wall, the viscous sublayer is highly perturbed by the presence of roughness, and in the fully rough regime it is entirely destroyed by the large turbulent mixing. This region, strongly affected by roughness elements, is called *roughness sublayer*.

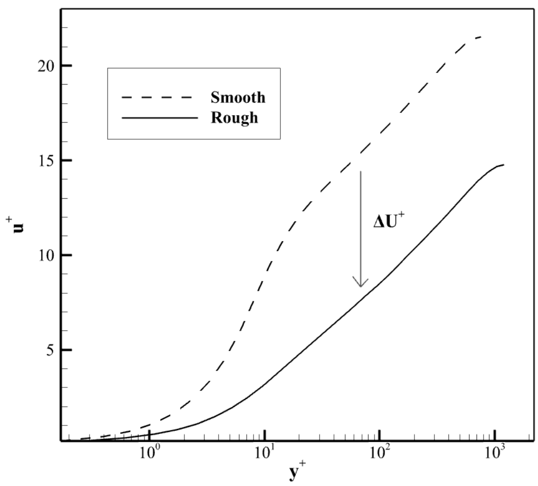

Figure 2: Dimensionless velocity profile over smooth and rough pipes plotted in wall variables.

DOI: 10.13009/EUCASS2022-6138

Later, Colebrook performed experiments on rough pipes and correlated the resulting pressure drop data with his well-known Colebrook and White equation [31]. Moody presented Colebrook's results in *Moody diagram*, which represents the Darcy friction factor f_D as a function of Reynolds number and relative pipe roughness h_s/D, in the range 0-0.05 [32].

Despite a significant number of experimental studies, most of the results reported in the literature mainly focus on roughness effects on momentum transport, while the field of thermal roughness effects is still quite unexplored and not fully understood. Over the years, different correlations of the Stanton number as a function of roughness height, Reynolds and Prandtl number have been derived [4, 7, 9]. Unfortunately, they all differ in their results, particularly for nonunitary Prandtl number fluids. In 1963, both Dipprey and Sabersky [7] and Owen and Thomson [8] independently proposed the *sublayer Stanton number* concept to account for heat transfer in roughness cavities. Rough walls can be imagined to consist of small cavities whose depth is of the order of the roughness height, in which eddies scour the surface and transport heat between the wall and the vigorous turbulent flow behind the roughness crests, forming the basic convective mechanism of heat transfer at the wall. These eddies are fed with vorticity from the streamwise flow away from the roughness elements and are subjected to frictional resistance at the solid surface where heat transfer between the fluid and the surface occurs by conduction in the conductive sublayer. Indeed, in the fully rough regime the viscous sublayer is destroyed while the conduction sublayer still exists in the thermal boundary layer. As a consequence, in the proximity of the wall, heat transfer is limited by conduction and depends on the properties of the fluid. Kays and Crawford [10] proposed a simplified formulation for the thermal law of the wall, in terms of nondimensional wall temperature T^+, to obtain the mean temperature profile on rough surfaces. The wall variable T^+ is defined as $T^+ = (T_w - T)/T_\tau$, where T_w is the wall temperature, T is the local flow temperature, $T_\tau = -q_w/(\rho c_p u_\tau)$ is the friction temperature, q_w the wall heat flux and c_p the fluid heat capacity. This simplified thermal law of the wall reads as:

$$T^+ = \frac{Pr_t}{\kappa} \log\left(\frac{32.6y^+}{h_s^+}\right) + \Delta T_0^+ \tag{2}$$

where Pr_t is the turbulent Prandtl number, κ is the von Kàrmàn constant and ΔT_0^+, analogous to the momentum wall roughness function ΔU^+, is a function of the non-dimensional sand grain height h_s^+ and of the fluid Prandtl number Pr.

The mentioned universal friction and thermal laws of the wall constitute a reference for any numerical approach of modeled turbulent flows. Along with them there is today a further reference thanks to the development of direct, i.e. nonmodeled, numerical simulations of turbulent flows (DNS). DNS allows to get high fidelity solutions of the flow around roughness elements for well-identified patterns as well as for randomly generated roughened walls [33, 34, 35]. These results are more useful for the verification and calibration of turbulence models than for use in practical applications, especially in the design phase because of their considerable computational cost. As a matter of fact, the correlation developed by Dipprey and Sabersky for fully rough surfaces gives good results with respect to DNS results in terms of Stanton number, further corroborating its use as representative of realistic heat transfer measurements [36, 37].

Modeled turbulence relies therefore on the law of the wall or on experimental/DNS data. The most common approach is to introduce roughness models into RANS solvers by the discrete element approach and the equivalent sand grain approaches. The discrete element approach solves equations for a flow spatially averaged over roughness elements [38, 39]. It accounts for roughness by extra terms in the flow equations, which represent the flow blockage and the drag and heat flux on roughness elements. However, the alteration of the equations generally precludes it use in general-purpose RANS solvers.

Therefore, the most popular and engineering approach is the so called *equivalent sand grain approach*, in which the real roughness height is linked to an idealized one through empirical correlations [24, 25] or pressure loss measurements, with respect to Nikuradse's experiments. Then, the equivalent sand grain height is introduced into the turbulence model to mimic the roughness effects by increasing the turbulent eddy viscosity in the wall region to obtain higher levels of skin friction and wall heat flux. Unlike the first two approaches, the equivalent sand grain one still preserves the Reynolds analogy. Therefore, it does not reproduce the differences between the increase in friction and heat transfer, with a consequent overestimation of heat transfer at high roughness [26, 40]. In this regard, Aupoix proposed a correction for the turbulent Prandtl number near the wall, based on the introduction of two additional parameters, besides the equivalent sand grain height, to characterize roughness thermal effects [26]. He used the discrete-element approach to generate a large database to calibrate the model. However, although Aupoix's correction improves heat transfer prediction, it needs parameters that are not easily accessible unless the roughness pattern is well identified. Aupoix's correction has been deduced for air (Pr=0.725) and mainly validated on external fluxes.

DOI: 10.13009/EUCASS2022-6138

3. Numerical model

The present analysis and model extension has been performed by an in-house preconditioned RANS flow solver based on a Godunov-type finite volume method which is second order accurate in space [41, 42]. Fluid thermodynamic properties are stored in a look-up table, thus the solver is capable to deal with any compressible fluid whose behavior is described by a generic equation of state. Turbulence is computed according to the one-equation model of Spalart-Allmaras [43], equipped with the extension developed by Boeing to account for wall roughness [40]. The latter is corrected to take into account thermal effects according to Aupoix's approach for external flows [26]. Parameters however have been recalibrated in the present study to fit experimental laws valid for pipes in the fully rough regime. The general expression for the correction is based on the introduction of a local value of the turbulent Prandtl number, which increases in proximity of the wall, with the purpose of decreasing the eddy conductivity and heat transfer to the wall. The correction of the turbulent Prandtl number takes the form:

$$Pr_t = Pr_{ts} + \Delta Pr_{tr} \tag{3}$$

where Pr_{ts} is the constant value assumed for smooth walls and assumed here as $Pr_{ts} = 0.9$ and ΔPr_{tr} is a correction which must be restricted to the wall region. Hence, ΔPr_{tr} can be expressed as:

$$\Delta Pr_{tr} = F \exp(-y/h_s) \tag{4}$$

where y is the normal distance from the wall. The exponential function aims to reduce the turbulent Prandtl number increase as moving away from the wall while the function F will be calibrated in the following on the basis of the available data. It will be shown in the following sections that F behavior is well described by a parabolic curve expressed as:

$$F(\Delta U^+) = a\Delta U^{+2} + b\Delta U^+ \tag{5}$$

The coefficients a, b have been found to depend on the fluid Prandtl number in the calibration phase, as will be discussed in the following.

This correction can be implemented in the model, computing the local value of ΔU^+ at runtime through the relation derived by Grigson [44]:

$$\Delta U^+ = \frac{1}{\kappa}\log\left(1 + \frac{h_s^+}{e^{1.3325}}\right) \tag{6}$$

where the expression of u_τ is in turn a local value that follows from the Boeing extension of the Spalart-Allmaras turbulence model [40]:

$$u_\tau = \frac{\tilde{\nu}}{\kappa(y + 0.03h_s)} \tag{7}$$

4. Model Calibration

To calibrate the model, RANS simulations are carried out for a uniformly heated axisymmetric channel whose operating conditions are changed to analyze a wide range of roughness levels and Reynolds numbers. The enforced boundary conditions are the following. At inflow, the static temperature T_i and the mass flow rate per unit area G are enforced, while at outflow the exit pressure p_e is prescribed. The wall boundary condition enforces a constant heat flux q_w towards the flow. The computational grid is clustered towards the wall to properly solve the boundary layer.

Calibration is made considering a fluid with constant properties (Pr = const) and comparing the numerical results with those of correlations. Before passing to test and calibrate the proposed thermal correction, grid resolution has been analyzed by grid convergence analysis using the Spalart-Allmaras model with the original roughness correction proposed by Aupoix and Spalart [40].

4.1 Grid Convergence

The grid refinement study has been performed with the number of cells of the coarse, reference and fine grids which are reported in Table 1. The resolution of the different grids is obtained while keeping the same clustering law. Therefore, the resulting values of the dimensionless wall distance y^+ changes according to the grid level. Grids have been designed as such to get the value of y^+ approximately equal to 1 for the reference grid for the following enforced flow conditions. Grid convergence test case is made assuming $Re = 2.7356\times10^4$ (Reynolds number based on the cross section diameter), $Pr = 6.033$, $h_s/D = 0.04$ and $L/D = 120$ to ensure a fully developed flow at the exit, and an imposed heat flux. Note that in the present conditions the viscous heating due to friction is negligible with respect to the enforced heat flux.

DOI: 10.13009/EUCASS2022-6138

Table 1: Number of cells for the three grid used for RANS simulations in the grid refinement study.

	N_x	N_r
Grid A (coarse)	30	7
Grid B (reference)	60	14
Grid C (fine)	120	28

Table 2: Relative pipe roughness levels h_s/D.

h_s/D	0.04	0.08	0.21

Results of grid convergence analysis are first presented in terms of the main bulk properties, temperature and pressure. Fig. 3 shows the evolution of the coolant pressure and the bulk temperature along the channel for the three grid levels. As expected, no effect of the mesh on the result of bulk temperature is detected, indicating that the energy balance is correctly satisfied, independently of resolution. Pressure evolution (Fig. 3b) shows a visible displacement at the coarsest level, as can be expected due to its extreme coarseness. However, variations between the reference and the fine grid are quite small, justifying the selection of *Grid B* as the reference one.

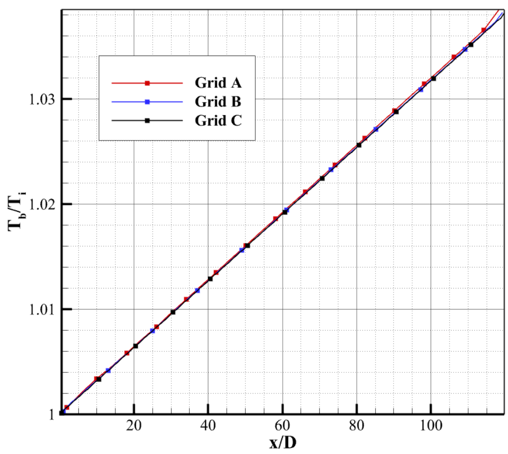

(a) Bulk temperature, T_b/T_i

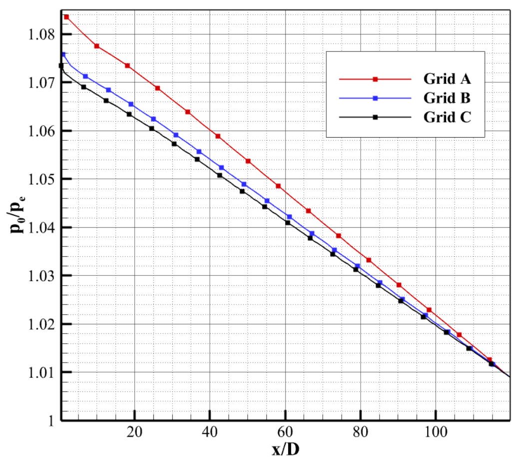

(b) Coolant total pressure, p_0/p_e

Figure 3: Grid convergence analysis for the evolution of the bulk temperature and pressure along the channel.

A further analysis of grid convergence has been performed on the evaluation of the Darcy friction factor f_D, considering three different relative pipe roughnesses, as reported in Table 2. Note that the extension of Spalart-Allmaras turbulence model developed by Boeing to account for wall roughness has been calibrated to give good results in terms of skin friction in the fully rough regime, where the Darcy friction factor f_D becomes almost independent of the Reynolds number.

The numerical value of the Darcy-Weisbach friction factor f_D is evaluated from the calculated streamwise pressure drop, according to:

$$\frac{dp_0}{dx} = -f_D \frac{\rho u_b^2}{2D} \tag{8}$$

and these results are compared with the Colebrook and White equation for rough pipes [45],

$$\frac{1}{\sqrt{f_D}} = -2\log\left(\frac{h_s}{3.71D} + \frac{2.51}{Re\sqrt{f_D}}\right) \tag{9}$$

In Fig. 4 the friction factor is presented as its ratio to the corresponding theoretical (empirical) value obtained by the Colebrook and White equation.

The friction factor behavior is based on the derivative of pressure, therefore it follows the trend of Fig. 3b. Fig. 4 allows to appreciate an almost second-order convergence of the value of f_D, which quickly reaches its asymptotic value. It is to note that the asymptotic value, starting from a value higher than the theoretical one, converges towards an underestimation.

Despite the extension of the Spalart-Allmaras turbulence model to account for wall roughness has been calibrated on external flows, results show a reasonable agreement with Eq. (9) for h_s/D=0.04 and 0.08 (about 5% shift).

DOI: 10.13009/EUCASS2022-6138

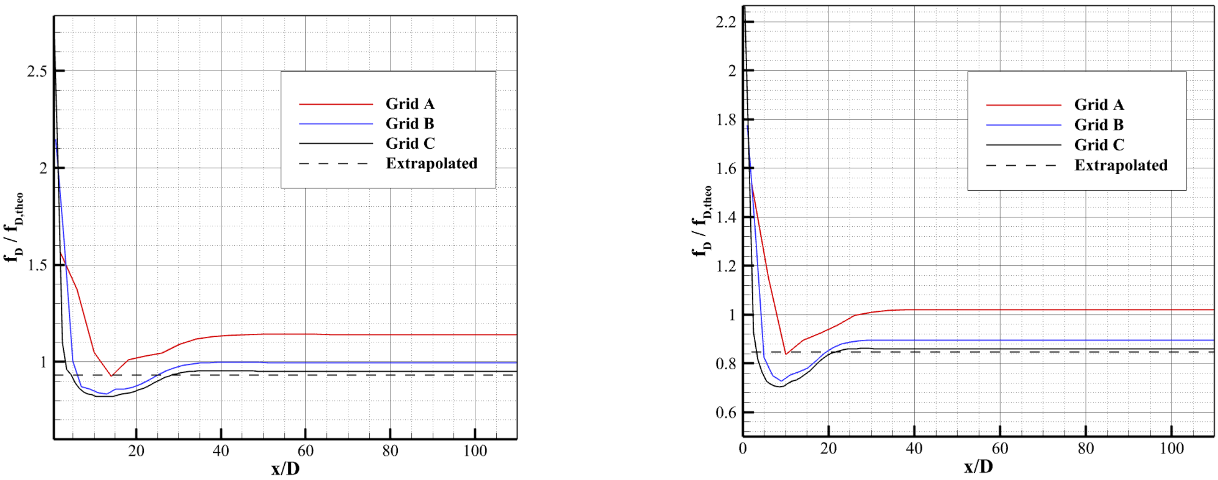

(a) h_s/D=0.04 (b) h_s/D=0.21

Figure 4: Grid convergence analysis for the Darcy friction factor.

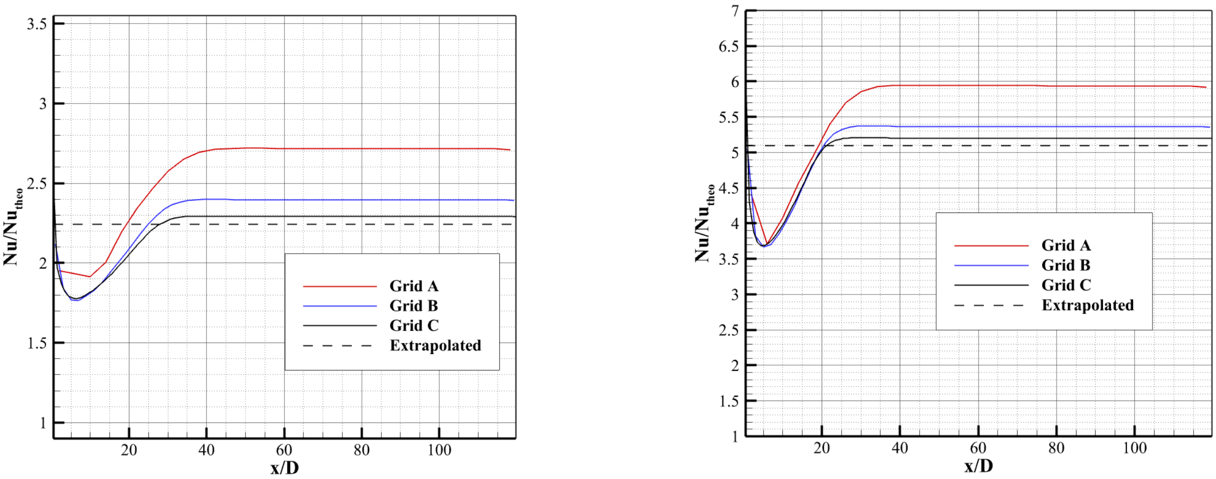

(a) h_s/D=0.04 (b) h_s/D=0.21

Figure 5: Grid convergence analysis for the Nusselt number.

On the other hand, when extremely high values of the relative pipe roughness are considered, the *Richardson* extrapolated value of f_D is considerably lower than the value of $f_{D,\text{theo}}$ obtained by solving for f_D the Colebrook and White equation, see Eq. (9). This is due to the fact that the extension of the Spalart-Allmaras turbulence model cannot take into account that in pipe flows the boundary layer growth is constrained by walls, and the relative pipe roughness can reach extreme values. In addition, the case of h_s/D=0.21 is well outside Colebrook's results reported in the Moody diagram, therefore, the reliability of the reference equation could also be questionable. Nevertheless, considered the out-of-range value of roughness and the wide range of applications of the model, the ~16% shift can still be considered a quite good approximation of the expected friction coefficient.

The grid convergence analysis has been then performed for the Nusselt number $Nu = hD/k$, where the convective heat transfer coefficient has been computed as:

$$h = \frac{q_w}{(T_w - T_{0b})} \tag{10}$$

Fig. 5 shows grid convergence results in terms of the ratio between the numerical computed Nusselt number and

DOI: 10.13009/EUCASS2022-6138

the theoretical reference equation of Dipprey and Sabersky [7], here presented in terms of the Stanton number:

$$St = \frac{f_D/8}{1 + \sqrt{(f_D/8)}\left\{k_f\left[Re(h_s/D)\sqrt{(f_D/8)}\right]^{0.2}(Pr)^{0.44} - 8.48\right\}} \tag{11}$$

with k_f=5.19.

The nearly second-order convergence seen for f_D is similarly appreciable for Nu. Differently, the asymptotic value of Nu is extremely far from the theoretical one and the error increases with increasing equivalent sand grain roughness height h_s, reaching a value greater than 400% for h_s/D=0.21. This is a main drawback of the equivalent sand grain roughness approach: if the equivalent sand grain roughness height is adjusted for skin friction, the predicted heat transfer results to be too high. Indeed, keeping the turbulent Prandlt number Pr_t constant and equal to 0.9, the turbulent conductivity k_t is directly derived once the turbulent viscosity μ_t is known. As a consequence, the different effects of roughness on skin friction and heat transfer are not reproduced and heat transfer results to be considerably overestimated at high roughness. Additionally, the error on heat transfer prediction dramatically increases with increasing equivalent sand grain roughness height. As a matter of fact, experiments have shown that there is a limit for any combination of Reynolds and Prandtl numbers beyond which an increase in roughness, while increasing the friction factor f_D will no longer increase the heat transfer coefficient h [7]. Indeed, when the roughness effect on friction becomes very large ($f_D/f_{D,0} > 4$, with $f_{D,0}$ the Darcy friction coefficient for smooth channels), no further increase in heat transfer is observed because the heat transfer resistance has become primarily a conduction resistance at the surface in the spaces between the roughness elements [10].

4.2 Thermal model calibration

To improve heat transfer prediction, the approach developed by Aupoix has to be recalibrated to fit the correlation of Dipprey and Sabersky in the fully rough regime, as done in [27]. As mentioned in Section 2, Aupoix's correction brings significant improvements in the heat transfer predictions, however the coefficients are not optimized with respect to channel experimental data as validation has been mainly done on external flows. Furthermore, he considered only air at moderate temperature, so Pr=0.725. As illustrated in Section 3, the correction to the turbulent Prandtl number is expressed by Eq. (4), where the function F must be now numerically determined to get the correlation results. To this end, for each different combination of h_s and Re considered, the value of F is artificially varied in the numerical model until the convective heat transfer coefficient in the fully developed region matches the theoretical value of Dipprey and Sabersky correlation.

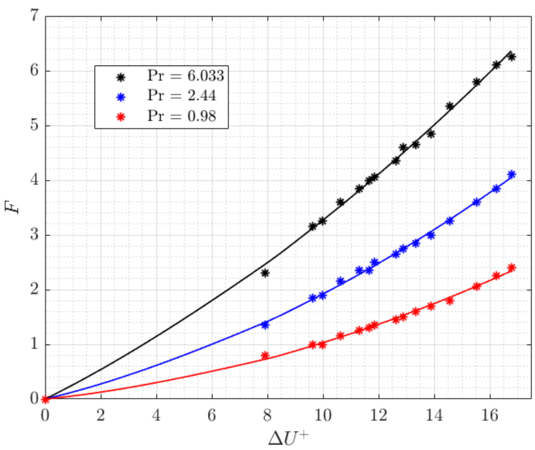

Figure 6: Fit of the F function for different Prandtl number

Once the values of F have been determined, they have been correlated with the corresponding values of the velocity shift ΔU^+, to characterize the dynamical effects of roughness. As the heat transfer is strongly dependent on the fluid Prandtl number, the correction has firstly been developed considering Pr = 6.033, representative of water. The effect of the Prandtl number on the correction has been then investigated considering Pr = 2.44 and Pr = 0.98, representative of the possible methane Prandtl number in LRE cooling channels (see Fig. 1).

DOI: 10.13009/EUCASS2022-6138

Fig. 6 shows the numerical values of F for the three different values of the Prandtl number considered, as related to the velocity shift ΔU^+. Data are fitted to characterize the curve, including the point $(\Delta U^+, F) = (0,0)$ as the correction must approach zero for smooth surfaces.

The result is that a good fitting is obtained by a parabolic curve, as anticipated in Eq. (5), with coefficient a, b which are functions of Pr:

$$a = (-2.346 \times 10^{-4})Pr^2 + (2.102 \times 10^{-3})Pr + 3.542 \times 10^{-3} \tag{12}$$
$$b = -(2.303 \times 10^{-3})Pr^2 + (5.588 \times 10^{-2})Pr - 3.043 \times 10^{-3} \tag{13}$$

5. Discussion

In this section the numerical results obtained using the present thermal correction for high roughness channels (THRC) are discussed. The effect of roughness on dimensionless velocity and temperature profiles has been analyzed; then the friction factor and Nusselt number values are shown compared to the theoretical values of a smooth pipe. Results obtained with THRC correction are also presented for: 1) experimental data of Dipprey and Sabersky at various Prandtl number; and 2) a test case representative of a liquid rocket engine cooling channel where methane is considered as a real fluid with variable properties.

Figs. 7a, 7b show the solutions obtained for the dimensionless velocity and temperature profiles (Pr = 6.03), respectively. The behavior of the dimensionless velocity profile at different roughness levels (Fig. 7a) shows that the effect of roughness is well mimicked using the Boeing extension of the Spalart-Allmaras turbulence model [40].

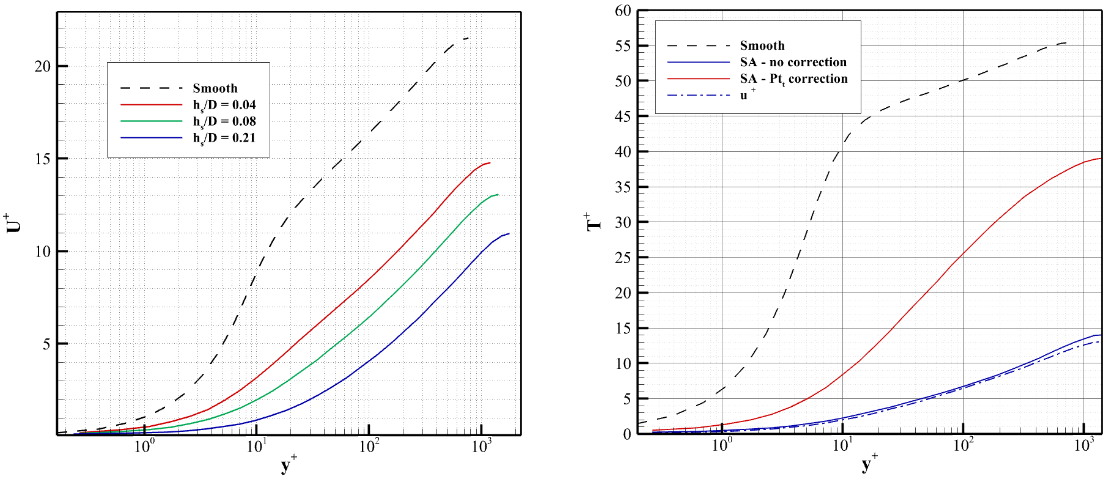

(a) velocity profile U^+ (b) temperature profile T^+: h_s/D=0.08

Figure 7: Smooth and rough dimensionless profiles as a function of the dimensionless wall normal coordinate y^+, Re=2.7356×10^4, Pr=6.03.

Indeed, roughness has a major effect in the vicinity of the wall, where the viscous sublayer ($0 < y^+ < 5$) is physically destabilized by the presence of roughness elements. In particular, in the fully rough regime, the viscous sublayer almost disappears entirely, accounting for the fact that the influence of viscosity on the hydrodynamic behavior of the flow is negligible. Above it, the logarithmic region is shifted downward by the quantity $\Delta U^+(h_s^+)$, but it retains its original slope [23].

The effect of THRC correction is clearly visible from the profiles of the dimensionless temperature T^+ obtained for Pr=6.03 with the assumption of smooth and rough pipe, respectively (Fig. 7b). When the turbulent THRC correction is not applied, and therefore the turbulent Prandtl number is kept constant and equal to 0.9, the temperature shift ΔT^+ with respect to the smooth curve is overestimated and follows the velocity profile. On the other hand, when the THRC correction is applied, it yields to a decreased heat transfer to the wall, and, accordingly, the increase in the wall temperature T_w results in a smaller temperature change ΔT^+.

Fig. 8 shows the increase in friction factor f_D caused by the roughness obtained for a flow with Re = 8.207×10^4. The numerical results of the reference grid are compared with the theoretical ones obtained using Eq. (9). Both the theoretical and numerical values are normalized with respect to the theoretical value of the corresponding smooth tube, (h_s/D=0).

DOI: 10.13009/EUCASS2022-6138

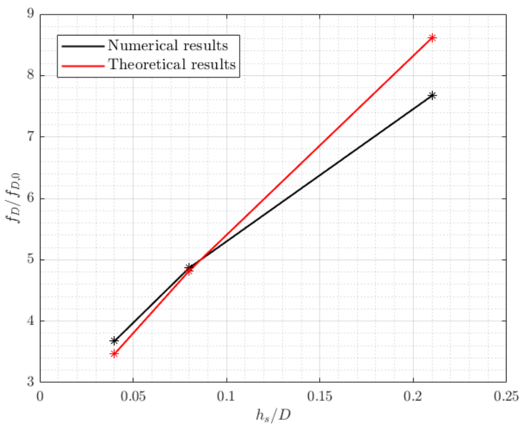

Figure 8: Friction factor ratio $f_D/f_{D,0}$ for the three different values of h_s.

Numerical results have been evaluated in the fully developed region where the friction factor is constant, being in the fully rough regime. The friction factor increases sharply with increasing equivalent sand grain roughness height and directly influences the pressure loss. As mentioned in Section 4, the numerical results agree well with the theoretical ones until extremely high values of the relative roughness of the pipe.

Results obtained with the THRC correction are shown in Fig. 9 in terms of the Nusselt number ratio, also normalized with respect to the theoretical value for smooth pipes Nu/Nu_0, as a function of the relative pipe roughness h_s/D. The reference value Nu_0 is computed by the Dittus-Boelter equation, while numerical results have been computed in the fully developed region. According to the experimental results of [46], the impact of roughness on heat transfer varies with Prandtl number, due to the corresponding variation of the thickness of the heat conduction sublayer. Additionally, the effect of roughness on heat transfer performance tends to flatten out for high values of the equivalent sand grain roughness height [10, 47]. The friction factor ratio $f_D/f_{D,0}$ discussed in Fig. 8 is also reported here for comparison. The comparison highlights the different behavior of friction factor and Nusselt number increasing with increasing roughness.

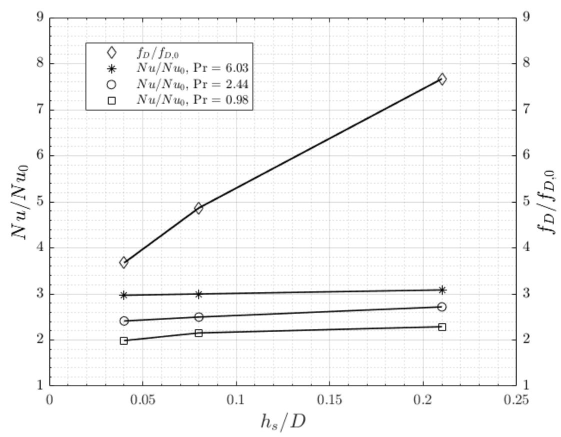

Figure 9: Nusselt number ratios for different values of h_s, Pr, Re=8.207×10^4.

This comparison is made more evident in Fig. 10 showing the ratio between heat transfer and friction factor increase caused by roughness normalized with respect to the smooth channel. Flattening of the heat transfer increase and continuous increase of friction factor lead to the decrease of their ratio at high values of the relative pipe ratio roughness. It is worth noting again that the effect of roughness is reduced for lower values of the Prandtl number.

The effect of the correction on the turbulent Prandtl number and fluid temperature distribution is shown in Figs. 11, 12, as compared to the original, non-corrected model, for h_s/D=0.08 and $Re = 2.7356 \times 10^4$. As mentioned in Section 3, the turbulent Prandtl number increases in the proximity of the wall in order to decrease the eddy conductivity. Accordingly, the fluid temperature increases in the wall region, as shown in Fig. 12.

Figure 13 shows the experimental data of Dipprey and Sabersky for a rough tube with a relative roughness

DOI: 10.13009/EUCASS2022-6138

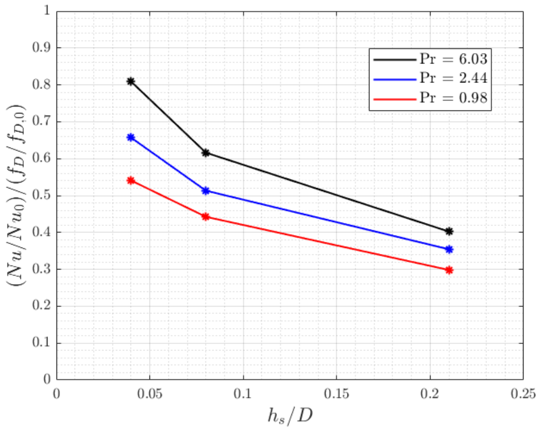

Figure 10: Nusselt number ratios for different values of h_s, Pr, Re=8.207×10^4.

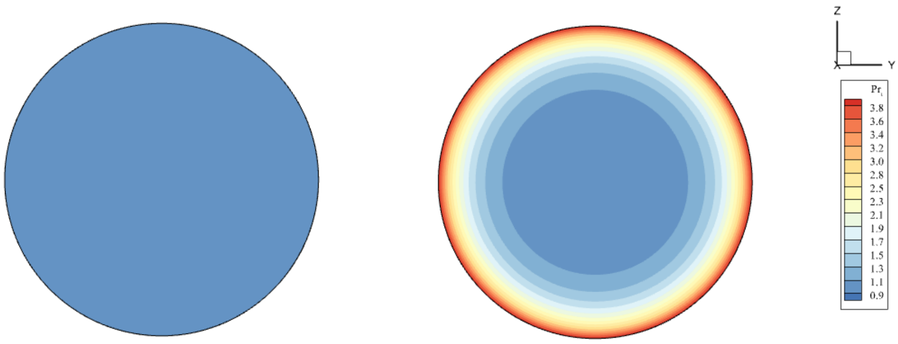

Figure 11: Turbulent Prandtl number: comparison between the original (left) and corrected (right) model.

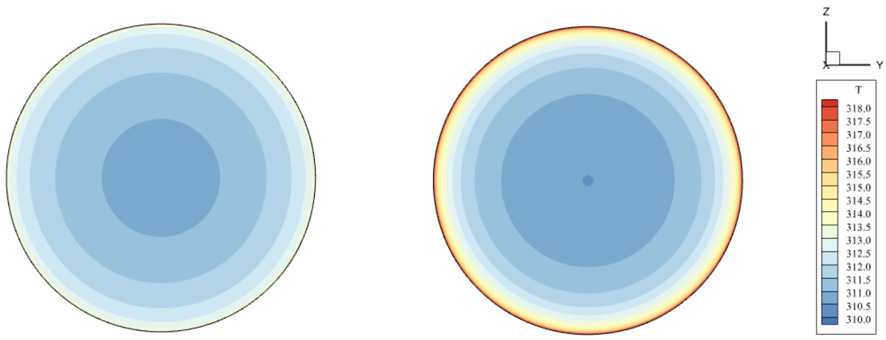

Figure 12: Fluid temperature: comparison between the original (left) and corrected (right) model.

h_s/D=0.049, $Re = 1.5 \times 10^5$ and Prandtl numbers equal to 1.2, 2.79, 4.38, 5.94, [7]. Results with the basic Spalart-Allmaras turbulence model strongly disagree with the experimental data, while numerical results obtained with the proposed correction are almost in line with the experiments.

During the study and the calibration of the correction, different simplifying assumptions have been made: the fluid properties are assumed to be constant and a constant uniform heat flux is enforced as a boundary condition. To test the correction outside of the simplifying hypothesis of constant fluid properties, simulations considering super-critical methane with variable properties have been carried out. Specifically, the 32-term modified Benedict-Webb-Rubin (mBWR) equation of state [48, 49] has been used.

DOI: 10.13009/EUCASS2022-6138

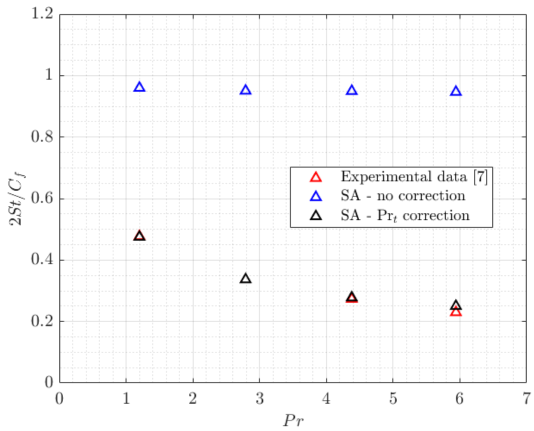

Figure 13: Heat transfer to friction ratios, h_s/D=0.049, Re=1.5×10^5 for different values of the Prandtl number [7]

The test case considered is categorized by h_s/D = 0.063, L/D = 250 and by an inlet velocity of 8.3 m/s.

A representative exit pressure of 150 bar has been assigned for the exit boundary condition. The inlet temperature is 250 K, and the Reynolds number reaches values up to 220000. Due to the variation of methane properties, the Prandtl number decreases from 1.45 to about 0.8, as shown in Fig. 14a. A constant heat flux of 1 MW/m^2 is imposed at the wall. Results are discussed in terms of the convective heat transfer coefficient and the Nusselt number, the latter reported in Fig. 14b.

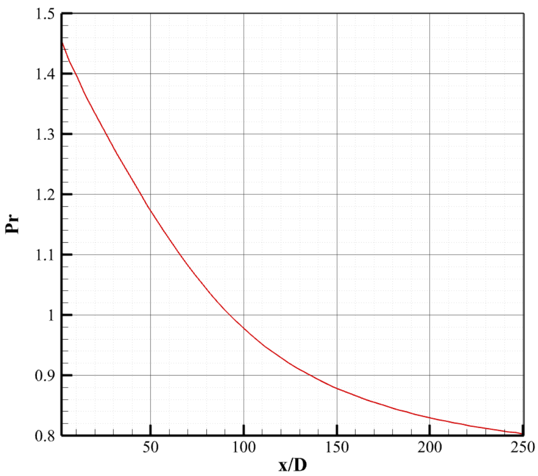

(a) Prandtl number evolution along the channel

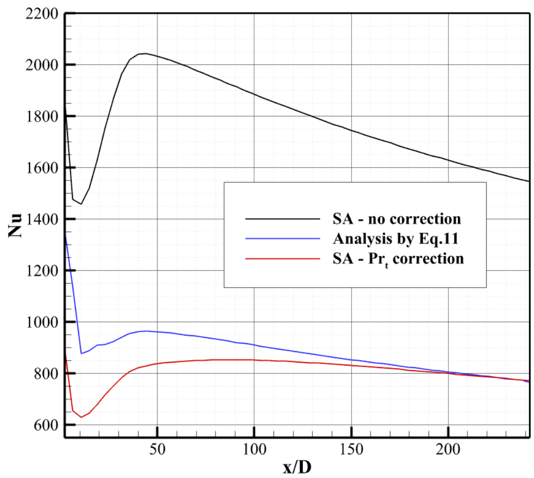

(b) Comparison of the Nusselt number along the channel computed through the original and corrected model

Figure 14: Variable properties super-critical methane.

The numerical results are compared with those obtained with the correlation of Dipprey and Sabersky. The correlation is used with bulk properties resulting from the numerical simulation. Results are interesting as they show the ability of THRC correction to handle properly the changes of properties. It is also interesting to discuss the discrepancy with respect to the Dipprey and Sabersky correlation that occurs in the first part of the channel. At a first glance, it can be surprising as the THRC correction has been calibrated on that correlation. Indeed, this discrepancy should be expected. The results are in good agreement in the region where the changes of the Prandtl number in streamwise and crosswise direction are smaller, while in the first part of the channel the Prandtl number changes are larger. In a region of large sensitivity of Prandtl number changes with temperature, or in correspondence of high heat fluxes leading to large changes of temperature in the crosswise direction, the hypothesis and data under which the Dipprey and Sabersky correlation is developed are no longer valid. In principle, the effect of roughness is mainly driven by the phenomena occurring in the vicinity of the wall, so local rather than bulk properties should be used. Accordingly, THRC correction takes into account local properties.

DOI: 10.13009/EUCASS2022-6138

In general, however, the THRC correction gives results that are in line with expectations, showing good agreement in a regime of constant properties. Such a result allows to consider the present correction as a general value correction for the application in circular cross-section cooling channels with high roughness. On the other hand, in case of changing properties, the availability of suitable experimental or DNS data would be of support to confirm that the predictions of the THRC corrected rough model of Spalart-Allmaras RANS closure are more robust than their calibration source.

6. Conclusions

THRC, a correction of the Spalart-Allmaras model aiming to predict realistic values of the convective heat transfer coefficient in high roughness cooling channels, has been implemented and calibrated with the correlation of Dipprey and Sabersky for circular cross-section channels. THRC is based on the basic extension of equivalent sand grain approach to account for wall roughness and on the turbulent Prandtl number increase in the wall region, which allows to decrease, in case of high roughness, the wall heat transfer which else would be highly overestimated. At present, the limited amount of experimental data only allowed to validate the correction on data for circular cross section pipe with a constant property flow. However, it can be expected that the THRC approach will improve the prediction for rectangular cross section channels and variable property flows as well.

7. Acknowledgments

Support by general funding of Italian Ministry of University and Research is acknowledged.

References

[1] A. Urbano and F. Nasuti, "Parametric analysis of cooling properties of candidate expander-cycle fuels," *Journal of Propulsion and Power*, vol. 30, no. 1, pp. 153–163, 2014.

[2] F. Nasuti and M. Pizzarelli, "Pseudo-boiling and heat transfer deterioration while heating supercritical liquid rocket engine propellants," *The Journal of Supercritical Fluids*, p. 105066, 2020.

[3] M. Leonardi, M. Pizzarelli, and F. Nasuti, "Analysis of thermal stratification impact on the design of cooling channels for liquid rocket engines," *International Journal of Heat and Mass Transfer*, vol. 135, pp. 811–821, 2019.

[4] W. Nunner, "Heat transfer and pressure drop in rough tubes," *AERE Lib/Trans.*, vol. 786, 1958.

[5] M. Niino, A. Kumakawa, N. Yatsuyanagi, and A. Suzuki, "Heat transfer characteristics of liquid hydrogen as a coolant for the LO2/LH2 rocket thrust chamber with the channel wall construction," AIAA Paper 82-1107, 1982. AIAA/SAE/ASME 18th Joint Propulsion Conference.

[6] M. Pizzarelli, F. Nasuti, and M. Onofri, "Coupled wall heat conduction and coolant flow analysis for liquid rocket engines," *Journal of Propulsion and Power*, vol. 29, no. 1, pp. 34–41, 2013.

[7] D. F. Dipprey and R. H. Sabersky, "Heat and momentum transfer in smooth and rough tubes at various prandtl numbers," *International Journal of Heat and Mass Transfer*, vol. 6, no. 5, pp. 329–353, 1963.

[8] P. R. Owen and W. R. Thomson, "Heat transfer across rough surfaces," *Journal of Fluid Mechanics*, vol. 15, no. 3, pp. 321–334, 1963.

[9] R. C. Martinelli, "Heat transfer to molten metals," *Trans. Am. Soc. Mech. Eng.*, vol. 69, pp. 947–959, 1947.

[10] W. M. Kays and M. E. Crawford, *Convective heat and mass transfer.* Tata McGraw-Hill Education, 3 ed., 1993.

[11] F. Morency and H. Beaugendre, "Comparison of turbulent prandtl number correction models for the stanton evaluation over rough surfaces," *International Journal of Computational Fluid Dynamics*, vol. 34, no. 4, pp. 278–298, 2020.

[12] F. Kerstens, A. Cervone, and P. Gradl, "End to end process evaluation for additively manufactured liquid rocket engine thrust chambers," *Acta Astronautica*, vol. 182, pp. 454–465, 2021.

DOI: 10.13009/EUCASS2022-6138

[13] P. Gradl and C. Protz, "Technology advancements for channel wall nozzle manufacturing in liquid rocket engines," *Acta Astronautica*, vol. 174, pp. 148–158, 2020.

[14] A. Patureau de Mirand, J. M. Bahu, and O. Gogdet., "Ariane next, a vision for the next generation of Ariane launchers," *Acta Astronautica*, vol. 170, p. 735 – 749, 2020.

[15] M. Rudnykh, S. Carapellese, D. Liuzzi, L. Arione, G. Caggiano, P. Bellomi, E. D'Aversa, R. Pellegrini, S. Lobov, A. Gurtovoy, and V. Rachuk, "Development of LM10-MIRA LOX/LNG expander cycle demonstrator engine," *Acta Astronautica*, vol. 126, pp. 364–374, 2016.

[16] J. Salotti, "Launcher size optimization for a crewed mars mission," *Acta Astronautica*, vol. 191, p. 235 – 244, 2022.

[17] M. Harris, "The heavy lift: Blue origin's next rocket engine could power our return to the moon," *IEEE Spectrum*, vol. 56, no. 7, p. 26 – 30, 2019.

[18] R. H. S. Hahn, J. Deeken, M. Oschwald, and S. Schlechtriem, "Turbine design and optimization tool for LUMEN expander cycle demonstrator," *Journal of Physics: Conference Series*, vol. 1909, p. 012053, may 2021.

[19] D. Kajon, D. Liuzzi, C. Boffa, M. Rudnykh, D. Drigo, L. Arione, N. Ierardo, and A. Sirbi, "Development of the liquid oxygen and methane M10 rocket engine for the Vega-E upper stage," EUCASS Paper 2019-315, 2019. 8th European Conference for Aeronautics and Space Sciences (EUCASS).

[20] M. Pizzarelli, F. Nasuti, M. Onofri, P. Roncioni, R. Votta, and F. Battista, "Heat transfer modeling for supercritical methane flowing in rocket engine cooling channels," *Applied Thermal Engineering*, vol. 75, pp. 600–607, 2015.

[21] M. Zhang and B. Sun, "Effect of artificial roughness on flow and heat transfer of transcritical methane," *International Journal of Thermal Sciences*, vol. 158, p. 106528, 2020.

[22] M. Shokri and A. Ebrahimi, "Heat transfer aspects of regenerative-cooling in methane-based propulsion systems," *Aerospace Science and Technology*, vol. 82, pp. 412–424, 2018.

[23] J. Nikuradse, "Laws of flow in rough pipes," Tech. Rep. NACA-TM-1292, 1950.

[24] R. Dirling, Jr, "A method for computing roughwall heat transfer rates on reentry nosetips," in *8th Thermophysics Conference*, p. 763, 1973.

[25] H. Schlichting and K. Gersten, *Boundary-layer theory*. Springer, 2016.

[26] B. Aupoix, "Improved heat transfer predictions on rough surfaces," *International Journal of Heat and Fluid Flow*, vol. 56, pp. 160–171, 2015.

[27] B. Latini, M. Fiore, and F. Nasuti, "Modeling liquid rocket engine coolant flow and heat transfer in high roughness channels," *Aerospace Science and Technology*, p. 107672, 2022.

[28] N. Saidi, M. Cerdoun, S. Khalfallah, and T. Belmrabet, "Numerical investigation of the surface roughness effects on the subsonic flow around a circular cone-cylinder," *Aerospace Science and Technology*, vol. 107, p. 106271, 2020.

[29] R. Szwaba, P. Kaczynski, and P. Doerffer, "Roughness effect on shock wave boundary layer interaction area in compressor fan blades passage," *Aerospace Science and Technology*, vol. 85, pp. 171–179, 2019.

[30] A. Zamiri, S. You, and J. Chung, "Surface roughness effects on film-cooling effectiveness in a fan-shaped cooling hole," *Aerospace Science and Technology*, vol. 119, 2021.

[31] C. F. Colebrook, T. Blench, H. Chatley, E. Essex, J. Finniecome, G. Lacey, J. Williamson, and G. Macdonald, "Correspondence. turbulent flow in pipes, with particular reference to the transition region between the smooth and rough pipe laws.(includes plates)," *Journal of the Institution of Civil engineers*, vol. 12, no. 8, pp. 393–422, 1939.

[32] L. F. Moody, "Friction factors for pipe flow," *Trans. Asme*, vol. 66, pp. 671–684, 1944.

[33] P. Orlandi, D. Sassun, and S. Leonardi, "Dns of conjugate heat transfer in presence of rough surfaces," *International Journal of Heat and Mass Transfer*, vol. 100, pp. 250–266, 2016.

DOI: 10.13009/EUCASS2022-6138

[34] M. Thakkar, A. Busse, and N. D. Sandham, “Direct numerical simulation of turbulent channel flow over a surrogate for nikuradse-type roughness,” *Journal of Fluid Mechanics*, vol. 837,R1, 2018.

[35] P. Orlandi and S. Pirozzoli, “Secondary flow in smooth and rough turbulent circular pipes: Turbulence kinetic energy budgets,” *Fluids*, vol. 6, no. 12, 2021.

[36] M. MacDonald, N. Hutchins, and D. Chung, “Roughness effects in turbulent forced convection,” *Journal of Fluid Mechanics*, vol. 861, pp. 138–162, 2019.

[37] J. Peeters and N. Sandham, “Turbulent heat transfer in channels with irregular roughness,” *International Journal of Heat and Mass Transfer*, vol. 138, pp. 454–467, 2019.

[38] H. W. Coleman, B. Hodge, and R. P. Taylor, “Generalized roughness effects on turbulent boundary layer heat transfer. a discrete element predictive approach for turbulent flow over rough surfaces,” tech. rep., Air Force Armament Laboratory AFATL-TR- 83-90, Mississippi State University, November, 1983.

[39] R. P. Taylor, H. W. Coleman, and B. Hodge, “Prediction of turbulent rough-wall skin friction using a discrete element approach,” 1985.

[40] B. Aupoix and P. Spalart, “Extensions of the spalart–allmaras turbulence model to account for wall roughness,” *International Journal of Heat and Fluid Flow*, vol. 24, no. 4, pp. 454–462, 2003.

[41] M. Pizzarelli, F. Nasuti, R. Paciorri, and M. Onofri, “Numerical analysis of three-dimensional flow of supercritical fluid in cooling channels,” *AIAA journal*, vol. 47, no. 11, pp. 2534–2543, 2009.

[42] M. Pizzarelli, F. Nasuti, and M. Onofri, “Coupled wall heat conduction and coolant flow analysis for liquid rocket engines,” *Journal of Propulsion and Power*, vol. 29, no. 1, pp. 34–41, 2013.

[43] P. Spalart and S. Allmaras, “A one-equation turbulence model for aerodynamic flows,” *La Recherche Aerospatiale*, vol. 1, pp. 5–21, 1994.

[44] C. Grigson, “Drag losses of new ships caused by hull finish,” *Journal of Ship Research*, vol. 36, no. 02, pp. 182–196, 1992.

[45] D. Brkic, “Review of explicit approximations of the Colebrook relation for flow friction,” *Journal of Petroleum Science and Engineering*, vol. 77, pp. 34–48, 2011.

[46] X.-w. Li, J.-a. Meng, and Z.-x. Li, “Roughness enhanced mechanism for turbulent convective heat transfer,” *International Journal of Heat and Mass Transfer*, vol. 54, no. 9-10, pp. 1775–1781, 2011.

[47] C. K. Stimpson, J. C. Snyder, K. A. Thole, and D. Mongillo, “Roughness effects on flow and heat transfer for additively manufactured channels,” *Journal of Turbomachinery*, vol. 138, no. 5, p. 051008, 2016.

[48] M. Benedict, G. B. Webb, and L. C. Rubin, “An empirical equation for thermodynamic properties of light hydrocarbons and their mixtures.,” *The Journal of Chemical Physics*, vol. 8, no. 4, pp. 334–345, 1940.

[49] B. Younglove and J. F. Ely, “Thermophysical properties of fluids. II. Methane, ethane, propane, isobutane, and normal butane,” *Journal of Physical and Chemical Reference Data*, vol. 16, no. 4, pp. 577–798, 1987.